Available online at www.sciencedirect.com

SciVerse ScienceDirect

Geochimica et Cosmochimica Acta 96 (2012) 230–246

Geochimica et Cosmochimica Acta

www.elsevier.com/locate/gca

The sources and sinks of CO_2 in caves under mixed woodland and grassland vegetation

Daniel O. Breecker [a,*], Ashley E. Payne [a,1], Jay Quade [b], Jay L. Banner [a], Carolyn E. Ball [a,2], Kyle W. Meyer [a], Brian D. Cowan [a,3]

[a] University of Texas at Austin, Department of Geological Sciences, United States
[b] University of Arizona, Department of Geosciences, United States

Received 26 April 2012; accepted in revised form 20 August 2012; available online 31 August 2012

Abstract

We measured concentrations and stable carbon isotope compositions of carbon dioxide in the atmospheres of three caves in central Texas and one cave in southern Arizona in order to identify CO_2 sources and sinks. The vegetation above the caves studied is either savannah (two caves, above which vegetation has been minimally disturbed) or discrete patches of grassland and woodland (two caves, above which vegetation has been highly disturbed). We tested two hypotheses concerning CO_2 in the cave atmospheres: (1) cave ventilation by tropospheric air is the primary sink for CO_2 and (2) CO_2 is primarily derived from the deepest rooting plants growing above the caves. Within caves, we monitored CO_2 at individual locations on monthly and daily time-scales and measured CO_2 along transects with increasing distance from the cave entrances. We also measured CO_2 in the pore spaces of soils under grasses and trees above each of the caves. We calculated $\delta^{13}C$ values of respired CO_2 ($\delta^{13}C_r$) for all gas samples using measured $\delta^{13}C$ values and CO_2 concentrations. We then identified the sources of cave CO_2 by comparing cave-air and soil CO_2 $\delta^{13}C_r$ values. At all locations in each Texas cave, CO_2 concentrations were highest (lowest) and $\delta^{13}C$ values were lowest (highest) during the summer (winter). Cave-air CO_2 concentrations consistently increased and $\delta^{13}C$ values consistently decreased with distance from the cave entrances. Similar but smaller magnitude seasonal variations in CO_2 concentrations occurred in the Arizona cave and no seasonal or spatial variation in the $\delta^{13}C$ of cave-air CO_2 was observed. The mean $\delta^{13}C_r$ values of CO_2 in soils under grass were 3.5–4.5‰ higher than the $\delta^{13}C_r$ values of CO_2 in soils under trees. In the caves under savannah, mean $\delta^{13}C_r$ values of cave-air CO_2 (−24‰ in both caves) were within 1‰ of the mean $\delta^{13}C_r$ values of CO_2 in soils under trees. In caves covered by large, contiguous areas of grassland, the $\delta^{13}C_r$ values of cave-air CO_2 were similar to grassland soil values during the summer and were intermediate between grassland and woodland soil values during the winter. The observed spatial and temporal variations in cave-air CO_2 are consistent with density-driven ventilation controlled by seasonal surface temperature changes as the primary sink for CO_2 in the Texas caves. The consistent agreement between soil and cave $\delta^{13}C_r$ values indicate that the same mixing and diffusion equations that are used to calculate $\delta^{13}C_r$ values of soil CO_2 also apply to cave-air CO_2. Our results suggest that the majority of CO_2 advects or diffuses into these caves from soils as a gas rather than being transported in aqueous solution. Measured $\delta^{13}C_r$ values and numerical production-diffusion modeling supports our hypothesis that the majority of gaseous CO_2 in these caves is derived from deeply rooted vegetation. The carbon isotope composition of groundwater and speleothem calcite used for paleoclimate records are therefore likely biased toward deeply rooted plants, even if sparsely present.

* Corresponding author.
E-mail address: breecker@jsg.utexas.edu (D.O. Breecker).
[1] Current address: University of California, Irvine, Department of Earth System Science, United States.
[2] Current address: University of Florida, Department of Geological Sciences, United States.
[3] Current address: Zara Environmental LLC, Manchaca, TX 78652, United States.

0016-7037/$ - see front matter © 2012 Elsevier Ltd. All rights reserved.
http://dx.doi.org/10.1016/j.gca.2012.08.023

1. INTRODUCTION

Caves facilitate the study of physical, chemical and biological processes in the deeper portions of the vadose zone. Caves also host speleothems, which preserve geographically widespread, high temporal resolution, and relatively long term (10^3–10^4 yrs) Quaternary paleoclimate records that can be dated accurately using U-series disequilibrium methods (see work by L. Edwards, e.g. Musgrove et al., 2001; Wang et al., 2001; Dykoski et al., 2005; and by others, e.g. Gascoyne, 1992; Richards and Dorale, 2003). We investigated spatial and temporal variations in CO_2 in cave-air to improve understanding of subsurface carbon cycle processes and thereby advance the use of speleothems as paleoclimate indicators.

Previous work has shown that CO_2 concentrations in some caves decrease when ambient atmospheric air temperature drops below cave-air temperature, causing outside air to sink into and displace air from caves (density-driven ventilation, e.g. Wigley and Brown, 1976). This decrease in cave-air pCO_2 drives degassing of CO_2 dissolved in cave waters and thus the precipitation of calcite according to the following reactions:

$$CO_{2(aq)} \rightarrow CO_{2(g)}$$

$$Ca^{2+} + 2HCO_3^- \rightarrow CaCO_3 + H_2O + CO_{2(aq)}$$

Calcite precipitation is suppressed and some speleothems may dissolve when ambient air temperature exceeds cave-air temperature causing ventilation to stagnate and cave-air CO_2 concentrations to increase. Seasonal changes in cave-air CO_2 concentrations are therefore thought to regulate calcite precipitation, and thus speleothem growth rate (e.g. Spötl et al., 2005; Banner et al., 2007; Baldini et al., 2008; Oster et al., 2012), which is commonly used as a proxy for rainfall. One of our objectives in the present study is to better understand cave CO_2 budgets as a means to improve this proxy with a better understanding of cave CO_2 budgets.

The carbon isotope composition of speleothem calcite is another speleothem-based climate proxy, which may record vegetation changes (e.g. Dorale et al., 1992, 1998; Hellstrom et al., 1998; Bar-Matthews et al., 1999; Genty et al., 2003; Denniston et al., 2007; Oster et al., 2009) and/or climate-related abiotic changes (e.g. Dulinski and Rozanski, 1990; Baker et al., 1997; Bar-Matthews et al., 1999; Mickler et al., 2006; Denniston et al., 2007; Oster et al., 2009). $\delta^{13}C$ values of speleothem calcite, however, are generally considered to be difficult to interpret and are not always reported in isotopic studies of speleothem calcite. A second objective of this study is to advance the interpretation of speleothem calcite $\delta^{13}C$ values by identifying the sources of carbon in cave-air CO_2 and by extension the source of carbon in epikarst water and speleothem calcite. To this end, we investigate the sources and sinks of cave-air CO_2 by monitoring the concentration and stable carbon isotope composition of cave-air CO_2 and of CO_2 in the pore spaces of soils dominated by grasses and by trees above caves in central Texas and southern Arizona.

2. BACKGROUND

Speleothems archive abundant paleoclimate information. The growth rate, trace element compositions, and stable isotope compositions of calcium carbonate and of fluid inclusions have all been used in numerous studies as paleoclimate proxies (Fairchild et al., 2006 and references cited therein). In particular, speleothem records from central Texas and southern Arizona (regions studied here) show that increased aridity in the southwestern US was associated with transition from the Pleistocene to Holocene warming in the North Atlantic during the last glacial period (Musgrove et al., 2001; Wagner et al., 2010; Meyer, 2011). In addition, the radiocarbon timescale has been calibrated by comparing U–Th and radiocarbon ages of speleothem calcite (Hoffman et al., 2010; Southon et al., 2012). Accurate radiocarbon timescale calibrations and proxy-based paleoclimate reconstructions require an understanding of the delivery and removal of CO_2 to and from caves. Specifically, this understanding is key to interpretation of speleothem carbon isotope variations as proxies for temporal shifts in vegetation (Dorale et al., 1992). Our contribution to this understanding in the present study builds on previous investigations summarized below of carbon cycling through soils, epikarst and caves and the influence that these processes have on speleothem formation and composition.

2.1. Cave CO_2 sinks

Ventilation is perhaps the best-studied process involved in the cycling of carbon through caves and is considered to be the primary mechanism of CO_2 removal from caves (de Freitas et al., 1982; Troester and White, 1984; Buecher, 1999; Spötl et al., 2005; Baldini et al., 2006, 2008; Banner et al., 2007). While cave-air ventilation may be controlled by many factors, two dominant mechanisms of removal include temperature-driven air flow and wind-driven air flow. The relative importance of these mechanisms varies according to the location and altitude of the entrances and the geometry and volume of the cave (Buecher, 1999; Fairchild et al., 2006; Batiot-Guilhe et al., 2007; Cowan et al., in press). Although surface temperatures fluctuate seasonally, temperatures within most caves remain nearly constant year-round. Seasonal overturn of cave-air occurs when surface temperatures decrease below cave temperatures, resulting in an unstable density gradient (e.g. Obir Cave, Austria, Spötl et al., 2005; Caves IS and NB of this study, Banner et al., 2007) Wind-driven ventilation operates according to the Venturi effect: seasonal changes in the direction of wind flowing past the cave entrance, and corresponding changes in wind strength, cause pressure changes below-ground resulting in air flow within the cave (Kowalczk and Froelich, 2010). Differences in the gradient and orientation of cave entrances as well as the dominant wind direction influence the cave-troposphere gas exchange. Shorter-term cave-air ventilation has been shown to be correlated to changes in atmospheric pressure, with fluctuations corresponding to thermally driven barometric tides (Baldini et al., 2006; Cowan, 2010). Similar to the ventilation mech-

anisms described above, the changes in the pressure gradient from the surface to the cave atmosphere drive flow in and out of caves resulting in decreases and increases in cave-air CO_2 concentrations, respectively.

2.2. Cave CO_2 sources

Potential sources of CO_2 in cave-air include: (1) deep geologic sources (magmatic/metamorphic), (2) decomposition of organic matter in caves, (3) local (above cave) soil respiration, (4) animal respiration, and (5) degassing from CO_2-rich groundwater (James, 1977; Troester and White, 1984). Deep sources are not considered in this study because the regions proximal to each cave are not magmatically or tectonically active. Tourism can increase CO_2 concentrations in cave-air by an order of magnitude (Baker and Genty, 1998 and references therein).

In many caves, the dominant sources of CO_2 are atmospheric air and soil respiration (Troester and White, 1984; Ek and Gewalt, 1985; White, 1988; Baldini et al., 2006, 2008). CO_2 from soil can be transported into the caves as a gas or dissolved in seepage waters. Ek and Gewalt (1985) concluded based on spatial variation of CO_2 concentrations that CO_2 produced in soils enters Belgian caves in seepage waters and as a gas through cracks in the epikarst. Spötl et al. (2005) reached the same conclusions for Obir cave, Northern Karawanken Mountains, southern Austria based on stable carbon isotope mass balance calculations. In contrast, stable carbon isotope mass balance suggests CO_2 enters Grotto di Ernesto cave, Asiago–Lavarone karst plateau, northeast Italy primarily as a gas rather than dissolved in seepage water (Frisia et al., 2011). Troester and White (1984) concluded based on similar seasonal variations in $CO_{2(g)}$ and $CO_{2(aq)}$ that CO_2 degassing from an underground stream is the primary source of cave-air CO_2 in Tytoona cave, Pennsylvania, USA.

2.3. Application of carbon isotope ratios to constraining sources and sinks

If soils are the dominant source of CO_2 in most caves, then the theory behind soil CO_2 and its carbon isotope composition should be considered when interpreting measured concentrations and $\delta^{13}C$ values of cave-air CO_2, and arguably also when interpreting measured $\delta^{13}C$ values of speleothem calcite. Soil respiration is the sum of CO_2 produced by root/rhizosphere respiration and by the microbial decomposition of organic matter. Respired CO_2 mixes with tropospheric CO_2 belowground in soil pore spaces and accumulates to concentrations that range from hundreds of ppmV to 20%, depending on temperature, water content, porosity, depth and other factors. Accumulation of respired CO_2 in soil pore spaces causes net diffusion of CO_2 along concentration gradients, eventually out of soils into the troposphere. $^{12}CO_2$ diffuses more rapidly than $^{13}CO_2$, which in addition to mixing with tropospheric CO_2, results in $\delta^{13}C$ values of soil CO_2 ($\delta^{13}C_s$, CO_2 in soil pore spaces) that are at least ~4.4‰ higher than the $\delta^{13}C$ value of respired CO_2 ($\delta^{13}C_r$, CO_2 emitted from the soil surface or produced within the soil) (Cerling, 1984; Cerling et al., 1991). At steady-state, the difference between $\delta^{13}C_s$ and $\delta^{13}C_r$ is ~4.4–5.0‰ when soil CO_2 concentrations are above ~10,000 ppmV. The difference between $\delta^{13}C_s$ and $\delta^{13}C_r$ increases as soil CO_2 concentrations decrease such that $\delta^{13}C_s$–$\delta^{13}C_r$ can be as large as 11‰ at 1000 ppmV. This effect complicates interpretations of the source of respired CO_2 based on $\delta^{13}C_s$ values alone. To circumvent this complexity, we solved the following equation derived by Davidson (1995) for $\delta^{13}C_r$:

$$\delta_s = 1.0044\delta_r + \frac{C_a}{C_s}(\delta_a - 1.0044\delta_r - 4.4) + 4.4 \quad (1)$$

where δ is the $\delta^{13}C$ value, C is the $^{12}CO_2$ concentration which can be approximated by the total CO_2 concentration, and the subscripts s, a and r represent soil, atmospheric and respired CO_2, respectively. We use the rearranged form of Eq. (1) to assess the relative influence of tree- and grass-dominated soils on cave-air CO_2.

3. STUDY SITES

Three caves located on the Edwards Plateau in central Texas and one cave located on the southeastern flank of the Santa Rita mountains in southern Arizona were studied: Inner Space Cavern (IS), Natural Bridge Caverns (NB) and Whirlpool Cave (WP) in Texas, and Cave of the Bells (COB) in Arizona. The land surfaces above some of the caves in this study have been affected by the construction of roads and buildings. The area on the surface around IS is the most urbanized of all locations; NB and WP are located in less disturbed settings; COB is remote and undisturbed. Satellite images of the distribution of vegetation above each cave are shown in Fig. 1. The passages extend down from the entrances of all the caves studied.

The Texas caves are situated within approximately 150 km of each other and have similar surface climate. Average surface air temperatures in central Texas are 36 °C in the summer (JJA) and 4 °C in the winter (DJF). The region generally experiences dry summers, with peak rainfall in the spring and, depending on tropical storm and hurricane tracks, in the fall as well. Soils above the Texas caves studied here are Lithic Haplustolls or Lithic Argiustolls and are thin (<30 cm) and rocky with fragments from the underlying bedrock (Godfrey et al., 1973; Cooke et al., 2007). Vegetation above NB is juniper and oak savannah whereas patches of grassland and woodland occur above the other Texas caves. Dominant tree species above the Texas caves are *Juniperus ashei* (ashe juniper) and *Quercus virginiana* (Texas live oak). Grasslands are dominated by *Bothriochloa ischaemum* (King Ranch bluestem) and *Carex planostachys* (Cedar Sedge) but also contain C_3 plants. Small percentages of the surfaces above each cave are covered by Texas Prickly Pear cactus (*Opuntia engelmannii*) a CAM plant. A study of roots exposed in caves on the Edwards Plateau (including NB studied here) demonstrated that *J. ashei* roots extend at least 8 m into bedrock and that *Q. virginiana* var. *fusiformis* roots extend to ~20 m (Jackson et al., 1999). No roots were found in caves below 25 m depth (Jackson et al., 1999). The majority of grassland root biomass likely occurs within the top

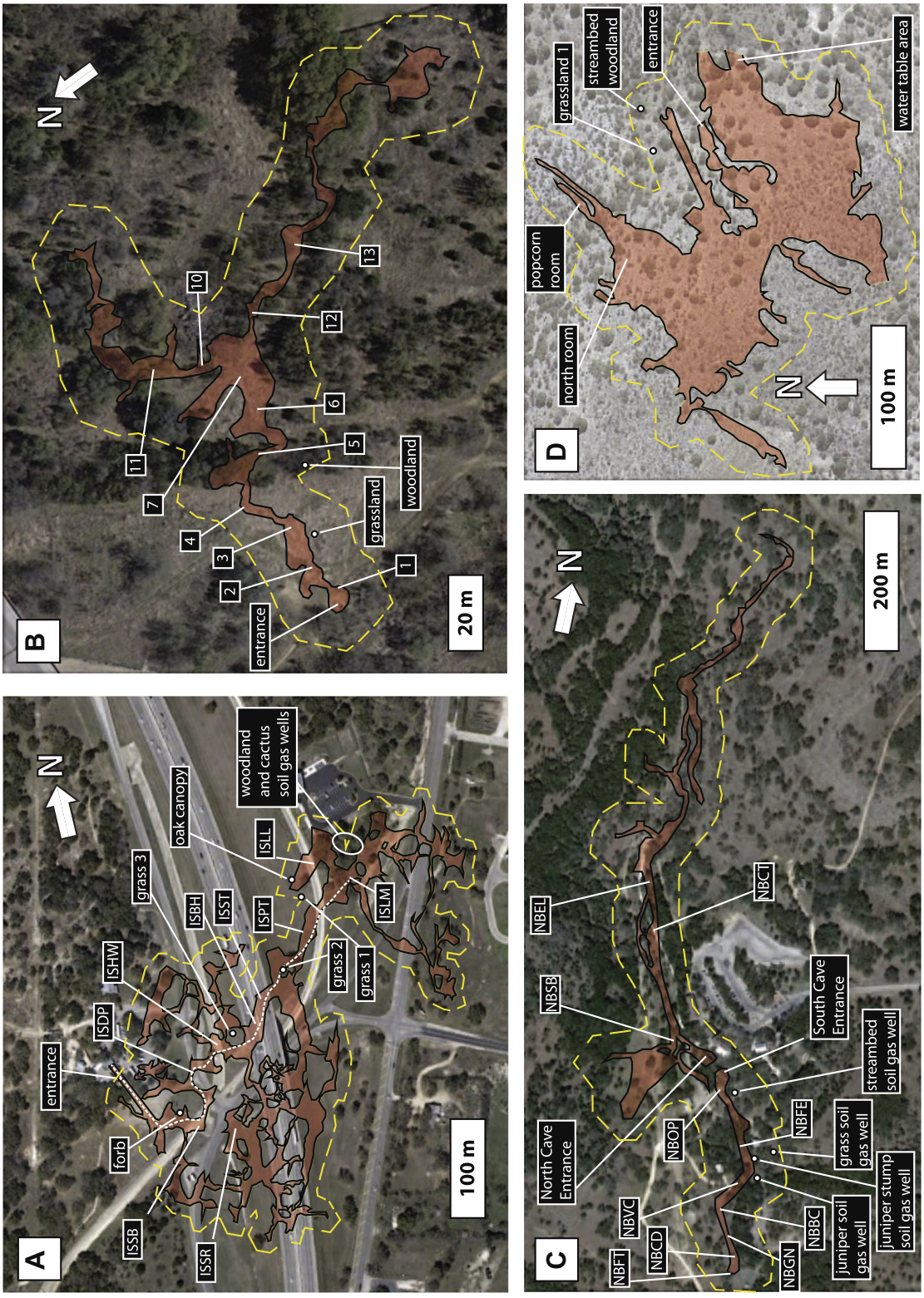

Fig. 1. Aerial view maps of the caves studied. (A) Inner Space Caverns (IS), (B) Whirlpool Cave (WP), (C) Natural Bridge Caverns (NB) and (D) Cave of the Bells (COB). The locations of the caves are shown in orange. Gas sample collection sites in the caves and in the soils above the caves are labeled; soil gas sampling locations are indicated by circles. The dashed yellow lines outline the area above each cave that is within one mean cave depth of the walls of each cave. The areas within the yellow dashed lines where used to calculate the fraction of the surface above the caves covered by tree canopies. IS and COB are covered by 15% tree canopy, WP by 50% tree canopy and NB by 60% tree canopy.

Table 1
Comparison of caves.

Cave name*	Location	Vegetation	Disturbance**	Radius of mean cave			
				Tourist cave	Entrance (m)	Depth (m)	Volume (m^3)
IS	Central TX	Patches of woodland and grassland	High	Yes	3	12	75,000
NB	Central TX	Oak and juniper savannah	Low	Yes	2	40	400,000
COB	Southern AZ	Oak and juniper savannah	Low	No	0.25	20	>40,000
WP	Central TX	Patches of woodland and grassland	High	No	1	10	22,000

* IS = Inner Space Cavern, NB = Natural Bridge Cavern, COB = Cave of the Bells, WP = Whirlpool.
** Degree of anthropogenic disturbance of vegetation.

50 cm; in nearby sandy loams, 80% of the herbaceous root biomass occurred in the top 60 cm of soil (Brown and Archer, 1990). Cactus roots typically do not extend below 30 cm with most roots in top 10 cm (Nobel, 1988).

Southern Arizona has a monsoon climate. Mean annual temperature at Cave of the Bells is about 14 °C with maximum air temperatures of 23 °C and minimum of 5 °C. COB is located beneath a hill flanked by seasonal streams. Soils above COB are shallow and gravelly Entisols and calcic Aridisols. The vegetation above the cave is characterized as juniper – oak savannah on the northeast-facing slope and as desert scrub on the southwest facing slope. *Juniperus deppeana* (alligator juniper) and *Quercus arizonica* (Arizona white oak) are the dominant tree species in the savannah, which also includes *Rhus choriophylla, Mimosa biuncifera*, *Bouteloua curtipendula* and *Bothriochloa barbinodis*. The dominant species in the desert scrub include *Viguiera sp.*, *Opuntia discata*, *Cowania mexicana*, *B. curtipendula*, and *Macrosiphonia brachysiphon*. There is a higher density of trees in and along the seasonal streams than on the hillslopes.

Characteristics of the caves studied are summarized in Table 1. Caves IS and NB are the two largest caves in this study. In both caves, public tours operate year-round and the natural entrances to both caves have been altered (Elliot and Veni, 1994; Banner et al., 2007). The caves contain ventilation shafts that are occasionally used in the summer months to decrease the build-up of CO_2 in order to make the environment comfortable for tourism (Cowan, 2010). IS has a total surveyed length of 4851 m, a maximum depth of 24 m, and a total volume of approximately 75,000 m^3 (Elliot and Veni, 1994; Cowan, 2010; Fig. 1A). The profile of the cave grades downward from the entrance; the vertical relief is 17 m from the entrance to the rear of the commercial path (Elliot and Veni, 1994). The cave consists of passages roughly 2 m across and numerous chambers greater than 2 m across. The transect sampled in this study traverses one of the larger of these chambers, where sites Borehole (ISBH) and Flowing Stone of Time (ISST) are located. No natural entrance to the cave exists. A large, gradually sloping artificial entrance to the cave faces the NW and is approximately 3 m in radius. NB has a length of 2621 m and a maximum depth of 76 m (Elliot and Veni, 1994; Fig. 1C). The vertical relief of the cave is much larger than that of IS (~50 m). The cave is composed of two caverns with separate entrances, Natural Bridge South (NBS) and Natural Bridge North (NBN). The approximate volume of NBS is 150,000 m^3 and of NBN is 250,000 m^3 (Cowan, 2010). Entrances to NBS and NBN are sealed by glass doors and face the WNW and SSE respectively. Vertical ventilation shafts to the surface are located in both caverns.

WP is much smaller in volume than the commercial caves. Passages within this cave are narrow and contain a few small chambers. Public access to WP is restricted. WP has a maximum depth of 13 m and a total volume of approximately 22,000 m^3 (Cowan, 2010; Fig. 1B). The nearly vertical entrance to the cave is covered by a gate that does not impede air flow. The profile of the cave beyond the initial drop at the entrance slopes gradually downward towards the east. The cave is Y-shaped with the majority of sampling sites for this study located within the first 1/3 of the cave (Fig. 1B). Passages are approximately 1 m in height and 4 m in width (Elliot and Veni, 1994). Active vadose drips were not observed in WP during the course of this study.

COB has the most complicated geometry of the caves studied. It has multiple levels and passages that lead up and down repeatedly, which likely limits density-driven ventilation. At least one passage in COB extends down to the water table. The entrance to COB is on a northeast facing hillslope and the passage leading into the cave constricts to an opening approximately 0.5 × 0.5 meters in cross section and approximately 1 m long, which might also restrict ventilation.

4. METHODS

Air sampling sites in the four caves were chosen along spatial transects with increasing distance into the caves. Cave-air samples were obtained on seasonal intervals, except at IS and COB where samples were collected on 4–12 week intervals. In addition to the monthly collection trips, cave-air samples were retrieved from IS every 2-h over a 24-h period between July 14th and July 15th, 2010. We collected samples in duplicate at each site, and the CO_2 concentration and temperature were measured using a portable Telaire 7001 CO_2 meter, with an uncertainty of approximately 5%.

Cave-air and soil-gas samples were collected using plastic disposable syringes and immediately injected into septum-capped, He-flushed 12 mL glass vials (Labco exetainers®) for transport to the laboratory. Cave-air was collected at least 5 m further into the cave than the rest of the group on each cave sampling trip. In addition, in order

to minimize any further anthropogenic effects on the cave-air samples, the person doing the sampling held their breath while taking the air sample. Air samples were also collected at the surface (tropospheric air) using this same procedure during each cave sampling trip. Human breath was sampled by blowing for five seconds into a needle penetrating the septum of a He-flushed exetainer®. A second needle was used as a vent to allow breath to displace helium in the vial.

Soil-gas wells of the design described in Breecker and Sharp (2008) were installed above IS, NB, WP and COB. The soil-gas wells were made of stainless steel tubing 40–50 cm in length and 5 mm in diameter. The bottom of the tubes were crimped shut and a slit, approximately 2 mm in width, was filed into the wall of the tubing near the crimp. Wells were inserted vertically into the soil above the caves using a battery-powered drill. A Swagelok ¼″ fitting and rubber septum were placed on the top end of the well to prevent any direct exchange of gas in the well with tropospheric air. Wells were installed in grasslands and woodlands (or under tree canopy in savannah) at depths ranging from 5 cm and 55 cm. Samples were collected by syringe through the rubber septum. A 3 mL (1 mL at COB) syringe was first flushed with gas from the well before samples were collected. A sample was then collected by extracting 3 mL of soil-gas from each well (0.2–2.0 mL for soil gas wells above COB) and injecting it into a He-flushed, septum-capped vial. Duplicate samples were collected from each soil-gas well to evaluate precision. Recoil of the syringe plunger indicated sub-atmospheric pressure in the well and required longer syringe collection times. This procedure ensured that tropospheric air did not contaminate the soil gas samples upon transfer from well to vial.

The soil and cave gas samples were analyzed using continuous flow gas chromatography/isotope ratio mass spectrometry (GC/IRMS). Within a week of collection an aliquot of each sample was transferred to a newly flushed exetainer® vial (no transfer was made for samples collected from COB soil gas wells, instead the entire sample was analyzed). Sample air was flushed from the vials in a He stream and directed through a liquid nitrogen cooled trap using a Gasbench II. The CO_2 in each aliquot was cryofocused and analyzed as a single pulse in continuous flow mode on a Delta Plus mass spectrometer. Carbon isotope compositions are expressed in the standard delta notation relative to VPDB. A CO_2-in-air standard calibrated to the VPDB scale in the Stable Isotope Laboratory at CU-INSTAAR in Boulder, Colorado (for calibration methods see Trolier et al., 1996) was used to calibrate an internal laboratory CO_2-in-air standard, which was analyzed alongside samples during each run.

Air samples for radiocarbon measurement were collected in evacuated, 1 L glass flasks. Air was drawn into the flasks from the soil (by connection to a manifold previously flushed with soil gas) or cave atmosphere through a quartz wool filter. The soil gas sample was collected in February 2009 from 55 cm depth in one of the grasslands above COB (grassland 1, Fig. 1). Cave-air was collected in November 2008 in the North Room and in February 2009 just above the water table (Fig. 1). CO_2 was separated from air cryogenically, passed through silver and copper wool to remove halogens and graphitized for analysis. The fraction modern carbon (fmc), as defined by Stuiver and Polach (1977), in each sample was determined in the Accelerator Mass Spectrometry laboratory at the University of Arizona.

5. RESULTS

The concentrations and $\delta^{13}C$ values of soil CO_2 and cave-air CO_2 measured in this study are presented in Tables 2–8. The $\delta^{13}C$ values of CO_2 in IS ranged from −17.7‰ to −8.6‰ and CO_2 concentrations ranged from 340 ppm to 8830 ppm. Spatial transects show a general trend toward decreasing $\delta^{13}C$ values with distance from the cave entrance (Fig. 2). $\delta^{13}C$ values of CO_2 from NBS range from −19.1‰ to −15.7‰ and CO_2 concentrations range from 750 to 13,700 ppm. $\delta^{13}C$ values of CO_2 from NBN range from −18.6‰ to −15.1‰ and CO_2 concentrations range from 750 to 3500 ppm. Whereas the maximum CO_2 concentrations at NBN were significantly lower than those of NBS, the range in the $\delta^{13}C$ values was comparable. $\delta^{13}C$ values of CO_2 from WP range from −21.0‰ to −14.9‰ and CO_2 concentrations range from 1400 to 17,800 ppm. $\delta^{13}C$ values of cave-air CO_2 within WP decrease with distance from the entrance. The $\delta^{13}C$ values of CO_2 in COB air vary by ±0.4‰ (1σ, $n = 21$, mean value = −19.2‰) with no spatial pattern detected. CO_2 concentrations in COB vary from ~8000 ppmV in the winter to ~12,000 ppmV in the summer.

The most complete time series of cave-air CO_2 measurements are from IS and COB. In IS, the lowest CO_2 concentrations and the highest $\delta^{13}C$ values occurred during the months of December, January and February of each year and the highest CO_2 concentrations and lowest $\delta^{13}C$ values were measured in June, July, and August (Table 2, Fig. 2). Similar seasonal changes were measured in Obir caves by Spötl et al. (2005). At IS, the magnitude of seasonal variation in CO_2 concentration and $\delta^{13}C$ values is largest nearest the entrance and decreases with distance into the cave. As a result the decrease of $\delta^{13}C$ values with distance from the cave entrance is larger during the winter than during the summer (Fig. 2). In COB, no seasonal pattern in $\delta^{13}C$ values occurs and variations in the $\delta^{13}C$ values and concentrations of CO_2 are smaller than they are in IS. The fmc in COB cave-air CO_2 was 0.94753 ± 0.00283 and 0.94744 ± 0.00014 in November 2008 and February 2009, respectively, which yielded a conventional radiocarbon age of 430 years BP. The fmc in the grassland soil at COB was 1.08365 ± 0.00016 in February 2009, which is indistinguishable from the present-day tropospheric CO_2 values.

Calculated cave-air CO_2 $\delta^{13}C_r$ values are listed in Tables 2–8 and are plotted in Fig. 3. Mean $\delta^{13}C_r$ values of cave-air CO_2 in IS, NB, WP and COB are similar (−24.2‰, −23.8‰, −23.1‰ and −23.9‰, respectively). Cave-air CO_2 $\delta^{13}C_r$ values vary seasonally in IS and WP; the lowest values occur in the winter or spring and the highest values in July or August. Cave-air CO_2 $\delta^{13}C_r$ values in NB and COB are less variable. When CO_2 concentrations in IS

Table 2
CO_2 concentrations and $\delta^{13}C$ values in IS cave-air.

Date	Outside air		ISSB			ISDP			ISHW			ISBH			ISST			ISLM			ISSR			ISLL		
	pCO_2	$\delta^{13}C$	pCO_2	$\delta^{13}C$	$\delta^{13}C_r$	pCO_2	$\delta^{13}C$	$\delta^{13}C_r$	pCO_2	$\delta^{13}C$	$\delta^{13}C_r$	pCO_2	$\delta^{13}C$	$\delta^{13}C_r$	pCO_2	$\delta^{13}C$	$\delta^{13}C_r$	pCO_2	$\delta^{13}C$	$\delta^{13}C_r$	pCO_2	$\delta^{13}C$	$\delta^{13}C_r$	pCO_2	$\delta^{13}C$	$\delta^{13}C_r$
7/3/2008	360	−9.2	781	−14.7	−23.7	1455	−13.0	−18.6	1260	−13.8	−20.0	1493	−13.8	−19.6	1654	−13.5	−19.0	2508	−13.9	−19.0	2483	−13.5	−18.5	2846	−17.0	−22.4
7/19/2008	392	−9.3	2878	−15.3	−20.6	2819	−15.3	−20.6	2968	−15.4	−20.6	3154	−15.3	−20.5	3143	−15.3	−20.5	4370	−16.3	−21.3				4478	−16.3	−21.3
9/23/2008	331	−10.0	1131	−14.7	−21.0	1680	−16.1	−21.9	1311	−15.8	−22.1	1708	−16.2	−22.0	1689	−16.1	−21.9	5307	−18.0	−22.8				4743	−17.6	−22.5
10/23/2008	300	−8.6	348	−10.5	−26.7	385	−12.2	−29.2	597	−13.1	−21.9	714	−12.7	−20.0	717	−14.2	−22.5	4293	−17.7	−22.7		−16.1		1467	−16.5	−22.8
12/6/2008	342	−9.9	339	−10.3		361	−11.2	−38.8	380	−11.2	−27.2	376	−12.5	−42.9	376	−12.1	−38.5	386	−12.9	−40.4	517	−14.3	−27.2	639	−15.6	−26.4
2/15/2009	320	−8.7	362	−11.0	−32.8	411	−14.7	−40.0	398	−12.3	−31.3	382	−11.7	−31.4	343	−13.1	−78.4	446	−12.1	−25.0	485	−13.8	−28.0	670	−15.3	−25.6
5/17/2009	244	−8.4				342	−9.2	−15.5	382	−11.3	−20.7	416	−11.8	−20.9	450	−10.0	−16.2	762	−12.8	−19.2	692	−13.0	−19.8	1080	−14.3	−20.3
8/10/2009	300	−7.9	2535	−15.6	−20.9	2974	−14.1	−19.1	3143	−15.3	−20.4	3840	−15.9	−20.9	4083	−15.9	−20.8	4862	−16.2	−21.1	5742	−15.8	−20.5	4575	−16.4	−21.3
10/4/2009	590	−10.2	1940	−15.6	−22.3	1910	−15.6	−22.3	2030	−15.6	−22.1	2330	−15.9	−22.1	2470	−15.9	−22.0	8830	−17.4	−22.2	4700	−16.3	−21.5	4540	−16.6	−21.9
6/29/2010	490	−9.4				2238	−16.6	−23.0							1652	−16.0	−23.1	3004	−17.0	−22.8	3048	−16.2	−21.8			
7/14/2010	543	−10.0				3319	−16.9	−22.6	3459	−16.7	−22.2				3429	−16.3	−21.8	4779	−17.6	−22.9						

are below 1500 ppmV CO_2, $\delta^{13}C_r$ values decrease with decreasing cave-air CO_2 concentration (Fig. 3D). During the 24 h study in IS, cave-air CO_2 concentrations reached a minimum at ISPT of 3500 ppmV at 07:00 (CST) and a maximum of 4400 ppm at 13:00 (CST) whereas $\delta^{13}C_r$ reached a maximum of −21.8‰ at 07:00 (CST) and a minimum of −22.8‰ at 13:00 (CST) (Fig. 4). Along transects into the cave, 1‰ changes in $\delta^{13}C_r$ values occur over <75 m and the position of these transitions shift in space diurnally (Fig. 4).

Soil CO_2 collected from gas wells above IS, NB, and WP on separate collection trips had $\delta^{13}C$ values ranging from −25.3‰ to −17.4‰ (Tables 3, 5 and 7; Fig. 3). $\delta^{13}C_r$ values for woodland and cactus soils above IS are higher in the summer (June, July, August, September) than in the spring (March) and fall (October) by up to 3.5‰. $\delta^{13}C_r$ values for grassland soils above COB vary from −22‰ during the winter to −19‰ in May and June. $\delta^{13}C_r$ values in the streambed woodland soil above COB are relatively constant (-23.9 ± 0.6‰, 1σ, $n = 12$). Mean $\delta^{13}C_r$ values of soil CO_2 under juniper trees are similar above NB, WP, and COB (−24.1‰, −23.5‰ and −23.9‰, respectively). Mean grassland soil $\delta^{13}C_r$ values are similar at IS, NB, WP, and COB (−20.3‰, −19.0‰, −19.7‰ and −20.5‰). There is a close agreement between cave-air CO_2 $\delta^{13}C_r$ values and tree-dominated soil $\delta^{13}C_r$ values at NB and COB. Cave-air CO_2 $\delta^{13}C_r$ values in IS and WP are similar to grassland $\delta^{13}C_r$ values during the summer and are intermediate between grassland and woodland values during the winter (Fig. 3). The mean $\delta^{13}C$ value of CO_2 in human breath was −21.5 ‰ (duplicate samples from five individuals, $1\sigma = 0.6$).

6. DISCUSSION

We apply our results to understanding the processes involved in carbon transport through karst and outline implications for interpretation of speleothem carbon isotope proxies. Cave-air CO_2 measured in this study is a mixture of two endmembers (as inferred by Banner et al., 2007): tropospheric air (~390 ppmV, −8.5‰ $\delta^{13}C$, VPDB) and an endmember with higher CO_2 and lower $\delta^{13}C$ values. The identification of tropospheric CO_2 as one of the two endmembers is supported by spatial trends of increasing $\delta^{13}C$ values and decreasing CO_2 concentrations toward the cave entrances and the near tropospheric values near the entrance of IS. Spötl et al. (2005) also interpreted cave-air CO_2 as a two-component mixture (tropospheric CO_2 and a 'light' endmember). The mixing relationships discussed below support density-driven ventilation as the primary sink for cave-air CO_2 and deeply rooted trees as the primary source of carbon in cave-air CO_2.

6.1. Evidence for ventilation

The spatial and temporal correlation between $\delta^{13}C$ values and concentrations of cave-air CO_2 are consistent with increased mixing ratios of atmospheric CO_2 in these caves during winter (compared with summer) and closer to the

Table 3
CO_2 concentrations and $\delta^{13}C$ values in IS soils.

Date	Outside air		Soil cactus 1 (28 cm)			Soil cactus 2 (11–26 cm)			Soil oak 1 (25 cm)			Soil oak 2 (7–22 cm)			Soil west (26 cm)		
	pCO_2	$\delta^{13}C$	pCO_2	$\delta^{13}C$	$\delta^{13}C_r$	pCO_2	$\delta^{13}C$	$\delta^{13}C_r$	pCO_2	$\delta^{13}C$	$\delta^{13}C_r$	pCO_2	$\delta^{13}C$	$\delta^{13}C_r$	pCO_2	$\delta^{13}C$	$\delta^{13}C_r$
3/27/2010	540	−9.8	9783	−20.4	−25.3				8414	−22	−27.1				10,290	−22	−27.0
6/29/2010	490	−9.4	6830	−18.1	−23.1				3178	−18.5	−24.5				23,216	−20	−24.0
6/27/2011			5375	−15.1	−19.8	13,720	−17.4	−21.9	17,554	−19.4	−23.9				22,527	−25	−29.8
8/16/2011			571	−11.3	−19.5	2875	−17	−22.4	741	−13.2	−21.5	1548	−17.4	−24.3	3772	−18	−22.9
9/9/2011			614	−12.8	−22.5	1398	−16.7	−23.7	517	−12.8	−26.0	987	−17.6	−26.9	1792	−19	−25.4
10/9/2011			2020	−17.7	−24.0	1341	−16.8	−24.2	2144	−20.8	−27.6	998	−17.9	−27.6	2249	−19	−25.3

Date	Outside air		Grassland 1 (10–25 cm)			Grassland 2 (9–24 cm)			Grassland 3 (9–24 cm)			Oak canopy savannah (5–20 cm)			Forb (4–19 cm)		
	pCO_2	$\delta^{13}C$	pCO_2	$\delta^{13}C$	$\delta^{13}C_r$	pCO_2	$\delta^{13}C$	$\delta^{13}C_r$	pCO_2	$\delta^{13}C$	$\delta^{13}C_r$	pCO_2	$\delta^{13}C$	$\delta^{13}C_r$	pCO_2	$\delta^{13}C$	$\delta^{13}C_r$
12/20/2011	409	−8.6	1498	−15.0	−21.7	1235	−13.3	−20.0	1132	−12.7	−19.3	3836	−20.5	−26.2	1212	−18	−26.6

Table 4
CO_2 concentrations and $\delta^{13}C$ values in NB cave-air.

Date			Natural Bridge South											
	Outside air		Step 92			NBOP			NBEP			NBVC		
	pCO_2	$\delta^{13}C$	pCO_2	$\delta^{13}C$	$\delta^{13}C_r$	pCO_2	$\delta^{13}C$	$\delta^{13}C_r$	pCO_2	$\delta^{13}C$	$\delta^{13}C_r$	pCO_2	$\delta^{13}C$	$\delta^{13}C_r$
6/11/2008	380	−8.5	1752	−18.7	−25.8	1684	−18.4	−25.6	5197	−18.6	−23.7	4701	−17.3	−22.4
3/8/2009	268	−8.6	870	−17.5	−25.7	762	−15.7	−23.8				2252	−18.5	−24.1
6/17/2010														

Date	Natural Bridge South													
	NBFE			NBBC			NBGN			NBCD			NBFT	
	pCO_2	$\delta^{13}C$	$\delta^{13}C_r$	pCO_2	$\delta^{13}C$	$\delta^{13}C_r$	pCO_2	$\delta^{13}C$	$\delta^{13}C_r$	pCO_2	$\delta^{13}C$	$\delta^{13}C_r$	pCO_2	$\delta^{13}C$	$\delta^{13}C_r$
6/11/2008	13,700	−18.4	−23.0	4748	−17.2	−22.3	4790	−19.1	−24.3	6651	−15.8	−20.6	5927	−18.6	−23.6
3/8/2009	1916	−18.1	−23.9	2374	−18.7	−24.3	2372	−18.5	−24.1	2568	−18.7	−24.2	3171	−18.9	−24.1
6/17/2010	4174	−17.3	−22.5							4609	−18.4	−23.6	4565	−18.5	−23.7

Date	Natural Bridge North								
	NBSB			NBCT			NBEL		
	pCO_2	$\delta^{13}C$	$\delta^{13}C_r$	pCO_2	$\delta^{13}C$	$\delta^{13}C_r$	pCO_2	$\delta^{13}C$	$\delta^{13}C_r$
6/11/2008	3398	−18.5	−24.1	3079	−17.7	−23.3	3213	−18.6	−24.2
3/8/2009	837	−15.4	−22.9	744	−15.1	−23.1	837	−16.6	−24.7
6/17/2010				3560	−17.6	−23.0			

entrances (compared with deeper regions of the caves). These observations confirm inferences made from CO_2 concentration time series that cave atmospheres are ventilated by tropospheric air during the winter (Banner et al., 2007; Cowan et al., in press). The magnitude of the effect of ventilation on cave-air CO_2 varies among the caves studied. Ventilation has a minor effect in COB compared with the other caves; the mixing ratio of tropospheric CO_2 in this cave is too small to have a measurable effect on cave-air CO_2 $\delta^{13}C$ values, even during the winter. The small area of the entrance and the undulating passages in COB likely limit density-driven ventilation. Ventilation has a larger effect in IS than in any of the other caves studied. The deep ventilation in IS may result from the large cross sectional area of the cave's entrance or possibly from wind blowing into the cave. Northerly winds accompany cold fronts moving into central Texas during the winter (NOAA) and IS is the only cave studied with a north-facing entrance. Given the resolution of the data from IS, however, it is unclear whether or not northerly winds enhance ventilation.

6.2. The source of carbon in cave-air CO_2

We determine the area above each cave (within the dashed lines in Fig. 1, which correspond to the projected area of each cave expanded in every direction by a distance equivalent to the depth of that cave) covered by grassland and by tree canopies using Adobe Illustrator to calculate the area of irregularly shaped polygons. Tree canopies cover 15% of the surface above IS and COB, 50% of the surface above WP and 60% of the surface above NB. The majority of the remainder of the surface above each cave is covered

Table 5
CO_2 concentrations and $\delta^{13}C$ values in NB soils.

Date	Juniper														
	10 cm			15 cm			21 cm			24 cm			34 cm		
	pCO_2	$\delta^{13}C$	$\delta^{13}C_r$	pCO_2	$\delta^{13}C$	$\delta^{13}C_r$	pCO_2	$\delta^{13}C$	$\delta^{13}C_r$	pCO_2	$\delta^{13}C$	$\delta^{13}C_r$	pCO_2	$\delta^{13}C$	$\delta^{13}C_r$
6/17/2010	3102	−18.5	−24.2	5578	−19.4	−24.5	8215	−20	−24.8	11,102	−19.9	−24.6	18,896	−20.1	−24.6
6/27/2011	2565	−18.1	−24.1	3037	−18.6	−24.3	6068	−19.3	−24.3	15,547	−20	−24.6	6284	−19.5	−24.5
8/19/2011	1104	−15.6	−23.6	1907	−17.1	−23.5	2482	−17.3	−23.2				4410	−18	−23.2
9/10/2011	840	−14.8	−24.3	1246	−16.8	−24.7	1528	−17.2	−24.4				2656	−18.5	−24.5
10/6/2011	1478	−16.3	−23.3	3858	−18.1	−23.4	4033	−18.5	−23.8				5402	−18.5	−23.6
	Grassland														
Date	6 cm			12 cm			18 cm			24 cm					
	pCO_2	$\delta^{13}C$	$\delta^{13}C_r$	pCO_2	$\delta^{13}C$	$\delta^{13}C_r$	pCO_2	$\delta^{13}C$	$\delta^{13}C_r$	pCO_2	$\delta^{13}C$	$\delta^{13}C_r$			
6/17/2010	1946	−11.9	−17.1	5403	−11.9	−16.5	6155	−12.8	−17.4	2961	−15.6	−21.0			
6/27/2011	2913	−13.4	−18.5	1544	−13.9	−20.0	5403	−14.3	−19.1	5952	−14.3	−19.0			
8/19/2011	580	−10.1	−17.5	730	−11.2	−18.5	765	−12	−19.8	791	−12.1	−19.7			
9/10/2011	619	−10.9	−19.0	807	−11.7	−18.9	890	−12.2	−19.3	1046	−12.5	−19.1			
10/6/2011	1823	−14.1	−19.9	2550	−14.6	−20.0	3038	−14.9	−20.1	3466	−15.3	−20.4			
	Streambed														
Date	11 cm			20 cm			23 cm			33 cm					
	pCO_2	$\delta^{13}C$	$\delta^{13}C_r$	pCO_2	$\delta^{13}C$	$\delta^{13}C_r$	pCO_2	$\delta^{13}C$	$\delta^{13}C_r$	pCO_2	$\delta^{13}C$	$\delta^{13}C_r$			
6/17/2010	8464	−16.5	−21.2	7936	−15.4	−20.1	8325	−15.4	−20.0	13,696	−16.4	−20.9			
6/27/2011	4390	−14.8	−19.7	5752	−15.7	−20.5	7535	−16.3	−21.0	9034	−17	−21.7			
8/19/2011	977	−14.1	−22.0	1368	−15.1	−21.9	1795	−15.6	−21.8	2619	−16.2	−21.8			
9/10/2011	950	−14.2	−22.3	1484	−15.4	−22.1	2000	−15.9	−21.9	2708	−16.5	−22.1			
10/6/2011	2203	−15.6	−21.4	3377	−16.6	−21.9	4004	−16.9	−22.1	5455	−17.2	−22.2			
	Juniper stump														
Date	10 cm			15 cm			22 cm			29 cm					
	pCO_2	$\delta^{13}C$	$\delta^{13}C_r$	pCO_2	$\delta^{13}C$	$\delta^{13}C_r$	pCO_2	$\delta^{13}C$	$\delta^{13}C_r$	pCO_2	$\delta^{13}C$	$\delta^{13}C_r$			
6/17/2010	1969	−17.3	−23.7	5443	−19.6	−24.7	15,120	−19.8	−24.4	20,090	−19.8	−24.3			
6/27/2011	2328	−17.7	−23.8	3106	−18.5	−24.2	4451	−18.9	−24.2	5330	−18.8	−23.9			
8/19/2011	539	−12.8	−27.4	760	−15.4	−26.6	1060	−16.7	−25.6	1375	−17.3	−25.0			
9/10/2011	576	−12.3	−24.0	728	−15	−26.4	985	−16.4	−25.6	1261	−17.2	−25.2			
10/6/2011	952	−15.7	−24.8	1218	−16.9	−25.0	1613	−17.6	−24.7	2022	−18	−24.5			

by grassland. The fraction of tree canopy coverage provides context for the carbon isotope measurements.

The source of carbon in soil CO_2 is better studied by considering $\delta^{13}C_r$ than $\delta^{13}C_s$ values (Cerling et al., 1991; Davidson, 1995). We suggest that if soils are the source of cave-air CO_2, then the advantage of studying $\delta^{13}C_r$ variations can and should be applied to cave-air CO_2 as well. Eq. (1) is appropriate for caves if CO_2 in caves or in the source region for cave-air CO_2 (i.e. soil or epikarst) reaches a steady-state exchange with the troposphere by diffusion. Calculation of $\delta^{13}C_r$ values allows comparison of the non-tropospheric components of cave-air CO_2 and soil CO_2 even if samples of these gases have different CO_2 concentrations. For instance, there is a consistent similarity between $\delta^{13}C_r$ values of cave-air CO_2 and tree-dominated soil CO_2 at COB (Table 8, Fig. 3B) but this similarity is not apparent if only the $\delta^{13}C$ values of CO_2 are compared (Table 8).

The consistent similarity between tree-dominated soil and cave-air $\delta^{13}C_r$ values and the consistent difference between grassland and cave-air $\delta^{13}C_r$ values suggests that the trees rather than grasses are the source of CO_2 in COB. A similar comparison considering two endmember mixing (grassland and tree-dominated soil) at NB also suggests a dominantly (>80%) tree source for cave-air CO_2 (Fig. 3A). Tree canopies cover 15% and 60% of the surface above COB and NB, respectively. Therefore, the influence of trees on cave-air CO_2 is disproportionately large in comparison with their surface coverage. Furthermore, the $\delta^{13}C$ value of cave-air CO_2 is not controlled by the percentages of C_3 and C_4 biomass on the surface above these caves. We suggest that trees (or decomposition of OM from trees) control cave-air CO_2 because trees root deeper than grasses in these ecosystems (e.g. Jackson et al., 1999). In some ecosystems (e.g. prairie) C_4 grasses are deeper rooted than C_3 forbs. Therefore the conclusions from our study of juniper and oak savannah that grasses have little influence on cave CO_2 $\delta^{13}C$ values may not apply in ecosystems without trees and should be tested in ecosystems in which trees are not as deeply rooted as they are in our study areas.

We numerically simulated CO_2 production and transport by diffusion in soil and epikarst to investigate whether theory supports our empirically-derived conclusion that

Table 6
CO_2 concentrations and $\delta^{13}C$ values in WP cave-air.

Date	Outside air		1			2			3			4		
	pCO_2	$\delta^{13}C$	pCO_2	$\delta^{13}C$	$\delta^{13}C_r$	pCO_2	$\delta^{13}C$	$\delta^{13}C_r$	pCO_2	$\delta^{13}C$	$\delta^{13}C_r$	pCO_2	$\delta^{13}C$	$\delta^{13}C_r$
10/23/2008	680	−13.2				5586	−21.0	−26.4				14,420	−16.9	−21.4
2/26/2009	314	−8.3				1397	−16.4	−23.0				2223	−17.4	−23.2
4/15/2009	370	−9.5				2220	−17.3	−23.2				3410	−19.4	−24.9
8/11/2009	393	−8.3	2151	−14.9	−20.7				2725	−15.9	−21.5			
8/1/2010						4841	−15.9	−20.8	5180	−16.4	−21.3			

Date	5			6			7			8		
	pCO_2	$\delta^{13}C$	$\delta^{13}C_r$	pCO_2	$\delta^{13}C$	$\delta^{13}C_r$	pCO_2	$\delta^{13}C$	$\delta^{13}C_r$	pCO_2	$\delta^{13}C$	$\delta^{13}C_r$
10/23/2008				13,860	−18.9	−23.5						
2/26/2009							5062	−18.0	−22.9			
4/15/2009										4020	−19.2	−24.5
8/11/2009	3451	−16.6	−22.0	4714	−16.8	−21.9						
8/1/2010	5017	−16.2	−21.1									

Date	10			11			12			13		
	pCO_2	$\delta^{13}C$	$\delta^{13}C_r$	pCO_2	$\delta^{13}C$	$\delta^{13}C_r$	pCO_2	$\delta^{13}C$	$\delta^{13}C_r$	pCO_2	$\delta^{13}C$	$\delta^{13}C_r$
10/23/2008	12,700	−19.0	−23.6	13,190	−19.0	−23.6	17,350	−19.4	−23.9	17,790	−18.4	−22.9
2/26/2009				4834	−18.1	−23.1	8174	−18.5	−23.2	9920	−18.7	−23.3
4/15/2009				4900	−19.4	−24.5				5500	−18.8	−23.8
8/11/2009				7812	−16.8	−21.6				12,300	−16.4	−21.0
8/1/2010	7347	−16.9	−21.6							15,592	−18.1	−22.6

Table 7
CO_2 concentrations and $\delta^{13}C$ values in WP soils.

	Grassland											
Date	10 cm			15 cm			20 cm			25 cm		
	pCO_2	$\delta^{13}C$	$\delta^{13}C_r$	pCO_2	$\delta^{13}C$	$\delta^{13}C_r$	pCO_2	$\delta^{13}C$	$\delta^{13}C_r$	pCO_2	$\delta^{13}C$	$\delta^{13}C_r$
8/1/2010	5735	−14.6	−19.3	8461	−15.1	−19.7	10,436	−15.4	−19.9	19,719	−15.6	−20.0
	Woodland											
Date	10 cm			15 cm			20 cm			25 cm		
	pCO_2	$\delta^{13}C$	$\delta^{13}C_r$	pCO_2	$\delta^{13}C$	$\delta^{13}C_r$	pCO_2	$\delta^{13}C$	$\delta^{13}C_r$	pCO_2	$\delta^{13}C$	$\delta^{13}C_r$
8/1/2010	6773	−18.1	−23.0	9461	−18.8	−23.6	8080	−18.6	−23.5	11,946	−19.4	−24.1

deeply rooted plants control cave-air CO_2 and therefore whether this conclusion might be applicable to ecosystems other than the ones studied here. We used the Forward-Time Central-Space (FTCS) method to solve Fick's second law of diffusion with a production term. Concentrations of CO_2 isotopologues were fixed at tropospheric values at the top of the soil and a zero gradient was established as the lower boundary condition. The effective diffusion coefficient for CO_2 was calculated as a function of free air porosity and pore space tortuosity (Bird et al., 1960; Quade et al., 1989). The diffusion coefficients for CO_2 isotopologues were calculated according to Craig (1954) and Jost (1960), following Cerling (1984). Errors associated with numerical approximation are insignificant at time steps $\leqslant 6$ s. Simulated CO_2 concentrations and $\delta^{13}C_s$ values were used to calculate apparent $\delta^{13}C_r$ values, which were then compared with empirical $\delta^{13}C_r$ values. We simulated a steady-state, 10 m deep CO_2 profile through soil and epikarst assuming that CO_2 with a $\delta^{13}C$ value of −19‰ is respired in the top 50 cm (typical soil depth on the Edwards Plateau is 20 cm) and CO_2 with a $\delta^{13}C$ value of −24‰ is respired at all depths below 50 cm (i.e. epikarst). Respiration rates were assumed to decrease exponentially with depth as shown in Fig. 5D such that 88% of the CO_2 respired in the soil–epikarst column came from the top 50 cm and the weighted mean $\delta^{13}C$ value of respired CO_2 was −19.6‰. In the simulation, less than 3% of the CO_2 respired came from below 4 m. The free air porosity was set at 0.5 from 0 to 0.5 m, at 0.3 from 0.5 to 4 m and at 0.1 below 4 m. This simple scenario was intended to test the relative influence on cave-air CO_2 of shallow (grassland soil) versus deep (trees roots in epikarst) respiration in areas where tree roots extend at depth beneath grasslands. Calculated apparent $\delta^{13}C_r$ values approach −24‰ (the prescribed tree root value and the mean observed cave-air value) at 10 meters, which is the approximate depth of the shallowest cave (WP) we studied. The simulated, steady-state, vertical gradient of apparent $\delta^{13}C_r$ values (Fig. 5B, dotted line)

Table 8
CO_2 concentrations and $\delta^{13}C$ values in COB cave-air and soils.

Date	Popcorn room			North room streambed woodland (61 cm)			Streambed woodland (61 cm)			Grassland 1 (55 cm)			Grassland 2 (70 cm)		
	pCO_2	$\delta^{13}C$	$\delta^{13}C_r$	pCO_2	$\delta^{13}C$	$\delta^{13}C_r$	pCO_2	$\delta^{13}C$	$\delta^{13}C_r$	pCO_2	$\delta^{13}C$	$\delta^{13}C_r$	pCO_2	$\delta^{13}C$	$\delta^{13}C_r$
9/5/2008							14,432	−20.0	−24.6	28,012	−15.6	−20.1	24,313	−16.7	−21.1
11/5/2008	9200	−19.0	−23.7							8488	−14.3	−18.9	8004	−15.6	−20.2
1/8/2009	9463	−19.2	−23.9	8703	−19.2	−24.0	2417	−18.0	−24.0	4792	−16.6	−21.6	6683	−16.9	−21.7
2/7/2009	8107	−18.8	−23.6	8327	−18.8	−23.6	2191	−17.7	−23.9	4221	−16.0	−21.1	5436	−16.7	−21.6
3/6/2009	8535	−19.1	−23.9	8595	−19.2	−23.9	2296	−17.5	−23.6	4759	−15.4	−20.3	4987	−16.1	−21.0
4/3/2009	8484	−19.5	−24.3	8221	−19.6	−24.4	1830	−17.7	−24.4	3758	−15.3	−20.4	5071	−16.2	−21.1
5/3/2009	9657	−19.1	−23.8	7439	−19.3	−24.2	1795	−17.0	−23.6	3761	−14.1	−19.1			
6/6/2009	9776	−19.6	−24.4	10,265	−19.5	−24.2	2542	−17.7	−23.6	4938	−14.0	−18.7	6099	−14.9	−19.6
8/1/2009							10,310	−19.3	−24.0						
1/16/2010	8238	−19.5	−24.3	8017	−19.6	−24.5	1462	−17.1	−24.4	2151	−16.1	−22.0	2323	−16.3	−22.1
4/24/2010	8421	−19.5	−24.3	8421	−19.9	−24.7	5178	−19.8	−25.0	8140	−16.4	−21.1	7048	−16.4	−21.2
5/22/2010	7892	−18.5	−23.3	7328	−18.3	−23.1	5065	−18.1	−23.1	8086	−13.9	−18.4	9760	−15.2	−19.8
7/28/2010	11,281	−18.8	−23.5	11,609	−18.9	−23.5	7436	−18.1	−22.9	11,128	−14.8	−19.3	12,403	−15.5	−20.0

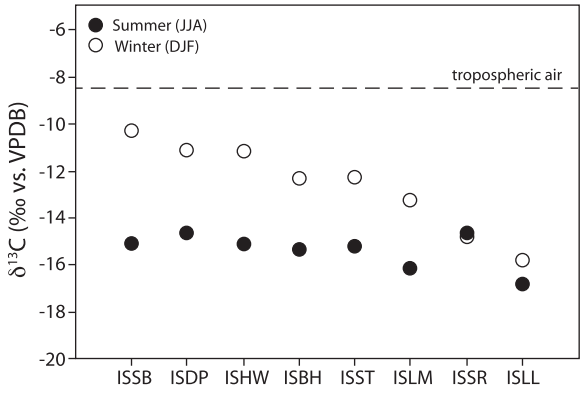

Fig. 2. Mean measured $\delta^{13}C$ values of cave-air CO_2 along transects into IS during our 18 month study. During the winter, the $\delta^{13}C$ values of cave-air CO_2 decrease from near tropospheric values at the cave entrance to −16‰ at the site furthest from the entrance. The gradient is shallower during the summer. These patterns are consistent with ventilation of IS by cold, dense tropospheric air during the winter. Locations of cave-air CO_2 sampling are shown in Fig. 1. IS refers to Inner Space in all sample names, the last two letters of the sampling are abbreviations as follows: SB = Soda Straw Balcony, DP = Drapery, HW = Hallway, BH = Borehole, ST = Flowing Stone of Time, LM = Lake of the Moon, SR = Squid Room, LL = Lunar Landscape.

demonstrates that respiration in the epikarst, rather than the surface soil, may control the $\delta^{13}C_r$ value of cave-air CO_2. Even low respiration in the epikarst can have a significant influence on cave-air CO_2 $\delta^{13}C$ values, especially if the effective diffusion coefficient for CO_2 in the deep epikarst is small. This conclusion is consistent with the speleogenesis model conceived by Wood (1985) in which low rates of deep vadose zone respiration (as opposed to soil respiration) are responsible for the high CO_2 concentrations in the deep vadose zone. Consideration of advection in numerical gas transport simulations would improve the application to ventilated caves.

Profiles of the fmc in CO_2 were also simulated using the FTCS method. Small fluxes of CO_2 from oxidation of passive soil carbon (hundreds to thousands of years old, e.g. O'Brien and Stout, 1978) deep in the epikarst might explain the relatively low radiocarbon specific activity in COB cave-air CO_2. The importance of old organic matter oxidation on speleothem carbon isotope compositions has been recently documented (Oster et al., 2010; Rudzka et al., 2011). One scenario that satisfies the observations made in this study is oxidation of ~1000 A.D. organic matter below 4 m, at a rate small enough that the weighted mean fmc of CO_2 respired in the entire soil and epikarst column is 1.075 (i.e. nearly equivalent to the observed value in the soil). The wetter-than-modern climate during the medieval warm period (e.g. Davis, 1994; Leavitt, 1994) might explain the presence of old organic matter at depth in the epikarst with $\delta^{13}C$ values similar-to-modern despite the higher-than-modern $\delta^{13}C$ values of preindustrial tropospheric CO_2. An old organic carbon source for cave-air CO_2 is consistent with the slow change in $\delta^{13}C$ values of speleothem calcite observed in the Cold Water Cave speleothem record (Dorale et al., 1992). Fractions of carbon from limestone in COB cave-air CO_2 that are larger than a couple of percent are difficult to explain given the close agreement between soil and cave-air CO_2 $\delta^{13}C_r$ values, unless soil CO_2 also contains limestone carbon. It is also possible that cave-air is equilibrated with a large volume of old groundwater (volume of air filled cave $\ll$ volume of groundwater). In this case, preferential recharge through woodland dominated streambeds followed by aging of carbon in the saturated zone could explain the observations. Measurements of the radiocarbon activity of drip water and the age of groundwater in this region would help distinguish between these two conceptual models. If the isotopic composition of CO_2 in COB air is controlled by groundwater, then the deeply rooted plants or the plants that grow in the streambeds must control the $\delta^{13}C$ value of groundwater dissolved inorganic carbon (DIC). This idea should be tested in other aquifers.

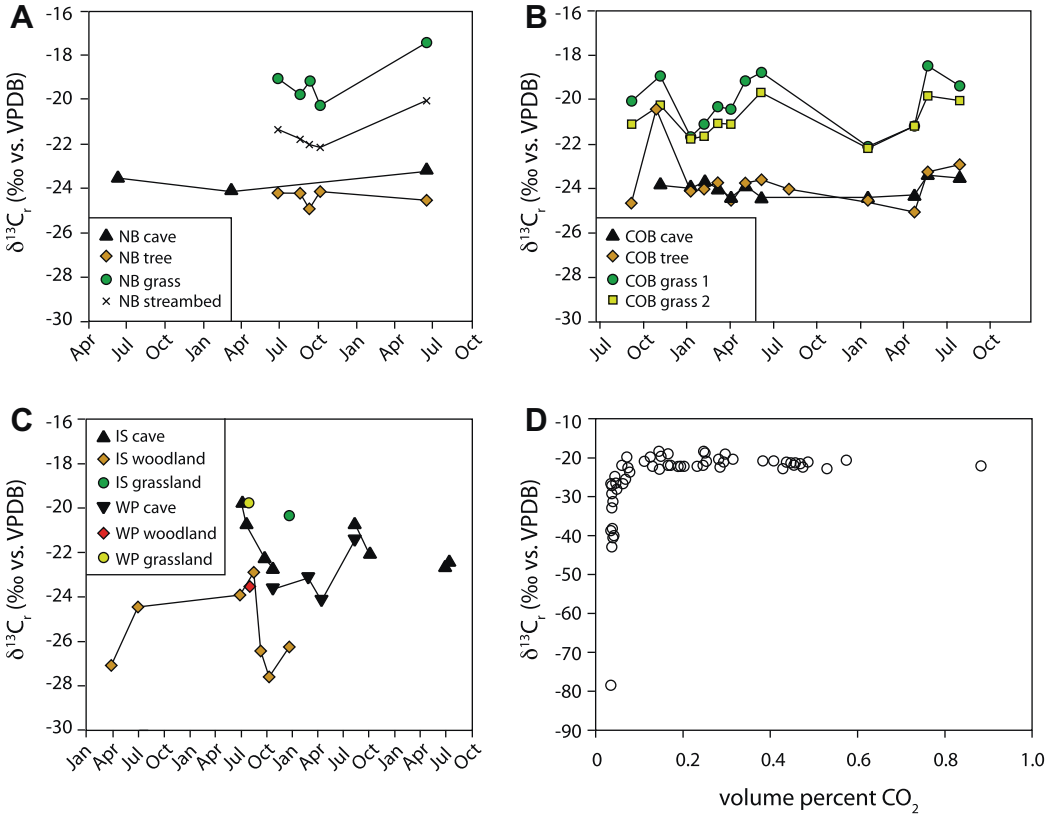

Fig. 3. Time series of calculated soil and cave-air CO_2 $\delta^{13}C_r$ values. Soils dominated by trees and by grasses are indicated by diamonds and by circles, respectively. (A) Natural Bride Caverns (NB). X's represent CO_2 in a gravelly streambed above the cave. (B) Cave of the Bells (COB). (C) Inner Space Caverns (IS) and Whirlpool Cave (WP). (D) Relationship between CO_2 concentrations and calculated $\delta^{13}C_r$ values for all sites in IS. Low $\delta^{13}C_r$ values that occur when cave-air CO_2 is below 1500 ppmV likely result from kinetic isotope fractionation during degassing of CO_2-supersaturated drip waters. $\delta^{13}C_r$ values for times when IS CO_2 was below 1500 ppmV (primarily winter) are therefore not included in the comparison with soil CO_2 in panel C. These results indicate that CO_2 in NB and COB comes primarily from tree-dominated soils whereas the CO_2 in IS and WP is primarily from grasslands during the summer and from both grasslands and woodlands during the winter. The uncertainty associated with the $\delta^{13}C_r$ values plotted is $\pm 0.2‰$.

If respiration of deep and possibly old organic carbon controls the carbon isotope composition of cave-air CO_2, then it probably also influences the carbon isotope composition of seepage waters and speleothem calcite. If true, then speleothems may provide records of the carbon isotope composition of deeply rooted plants and/or the presence/absence of deeply rooted plants. In addition, radiocarbon calibrations should take into account that carbon may have aged in the soil or epikarst for a 1000 years or longer before being incorporated into speleothem calcite, even in the absence of incorporation of limestone carbon. Measurements of the carbon isotope composition of cave waters and harvested cave calcite are required to test these ideas.

Calculated $\delta^{13}C_r$ values of cave-air CO_2 in IS during the winter (-25 to $-80‰$, Table 2) are too low to be interpreted as soil-derived. Instead, the low $\delta^{13}C_r$ values that occur when cave-air CO_2 concentrations are below 1500 ppmV CO_2 (Fig. 3D) are likely controlled by preferential degassing of $^{12}CO_2$ from CO_2-supersaturated drip water (Spötl et al., 2005). Therefore, water likely transports a substantial fraction of CO_2 into IS during the winter. Unfortunately, this process obscures the determination of carbon sources using winter $\delta^{13}C_r$ values of cave-air CO_2 in IS. The sources of cave-air CO_2 in IS can, however, be assessed at other times of year.

During the summer, $\delta^{13}C_r$ values of cave-air CO_2 in IS and WP are similar to $\delta^{13}C_r$ values of grassland soil CO_2 measured at WP and NB (we did not measure $\delta^{13}C_r$ values of grassland soil CO_2 at IS during the summer). We therefore suggest that grasslands are the primary source for cave-air CO_2 during the summer at IS and WP, which is consistent with the large area of contiguous grassland above these caves. In comparison to IS, the savannah ecosystem above COB has a similar percentage of tree cover (~15%), but the trees are more evenly distributed at COB whereas at IS the trees mostly occur in woodlands located over distal corners of the cave (Fig. 1). The trees are more clustered above WP than COB and a large patch of grassland occurs above the region within WP where most of the cave-air CO_2 samples were collected (Fig. 1). Our one-dimensional numerical simulation indicates that deeply rooted trees will dominate the contribution to cave-air CO_2 if they grow close enough together. However, larger distances between trees, like those at IS and WP, should increase the influence of shallower

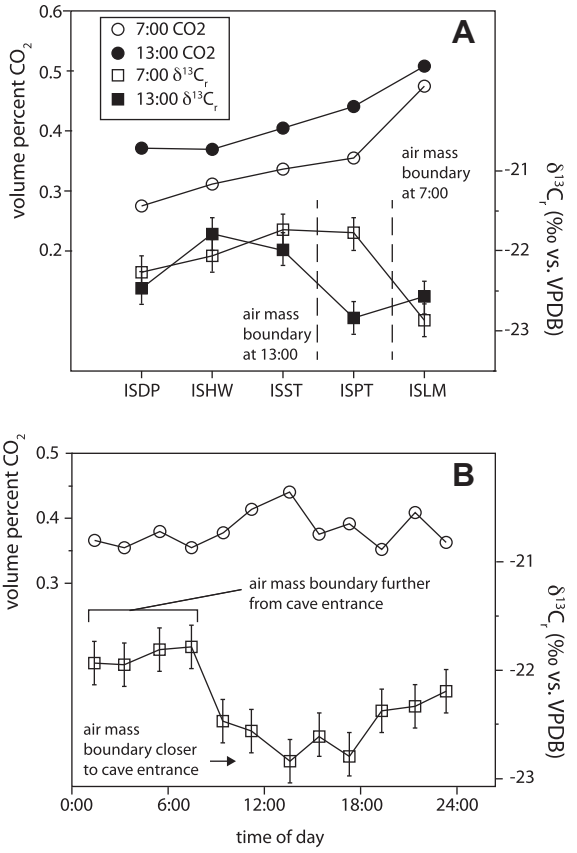

Fig. 4. CO_2 concentrations and $\delta^{13}C_r$ values of cave-air CO_2 in IS during the July 2010 24-h study. (A) Comparison of transects into IS during the morning and early afternoon. (B) Diurnal variations in the concentration and $\delta^{13}C_r$ value of cave-air CO_2 at sampling site ISPT. Air masses (boundaries defined by dotted lines in A) with distinct $\delta^{13}C_r$ values move back and forth across ISPT with a period of approximately 24 h. This process is not recorded by cave-air CO_2 concentrations alone. ISPT = Inner Space Painting.

grassland soil respiration on the $\delta^{13}C$ value of cave-air CO_2. A two-dimensional CO_2 production and transport model would help test this idea.

A decrease of ~3‰ in the $\delta^{13}C_r$ value of cave-air CO_2 occurs from July through October in IS. This decrease is not related to kinetic fractionation during degassing, as demonstrated by the poor correlation between $\delta^{13}C_r$ values and cave-air CO_2 concentrations during this time period ($r^2 = 0.02$, $p = 0.77$, $n = 8$). The decrease in $\delta^{13}C_r$ values may instead result from an increase in the relative contribution of woodland soil CO_2 to the cave, a decrease in the $\delta^{13}C$ value of CO_2 respired in all soils above the cave, or perhaps both. The difference between $\delta^{13}C_r$ values of cave-air CO_2 in WP and IS on the same days in October and August were 0.9‰ and 0.8‰, respectively (Fig. 3C). The $\delta^{13}C_r$ values of cave-air CO_2 in WP may therefore be used to approximate the source of CO_2 in IS during the winter. Comparison of winter $\delta^{13}C_r$ values of cave-air CO_2 in WP (+1‰ to account for the difference observed in October and August) with winter $\delta^{13}C_r$ values of grassland and oak canopy soil CO_2 above IS suggests there is a 40% contribution of CO_2 from trees. Although this is a smaller fraction than the contribution from trees at COB and NB, it is large in comparison with the fraction of the surface covered by tree canopies. Further monitoring is required to better quantify the contribution of trees to the CO_2 in IS.

Human breath is another potential source of CO_2 in caves. The average $\delta^{13}C$ value of CO_2 in breath of North Americans is between −21‰ and −20‰ (Schoeller et al., 1980), which is intermediate between $\delta^{13}C_r$ values of grassland and tree-dominated soil CO_2 and is similar to $\delta^{13}C_r$ values of mean cave-air CO_2 in IS during the summer-fall transition. The $\delta^{13}C$ values of CO_2 in human breath measured in this study are similar to the values reported by Schoeller et al. (1980) and are significantly higher than the $\delta^{13}C_r$ value of cave-air CO_2 in COB, NB and WP ($p < 0.002$ in each case). Furthermore, $\delta^{13}C_r$ values of cave-air CO_2 observed at NB (a tourist cave) are similar to values at COB and WP (wild caves with relatively few visitors). Therefore human breath is probably not responsible for the tree-biased $\delta^{13}C_r$ values of cave-air CO_2 in the caves we studied. High-resolution temporal variations in cave-air CO_2 concentrations in IS do not peak during the passage of tour groups (Cowan, 2010), further supporting the conclusion that human breath is of minor importance for CO_2 in these caves.

6.3. CO_2 transport into caves

The mechanism of CO_2 transport into caves has not been widely studied. The similarities between $\delta^{13}C_r$ values of soil CO_2 and cave-air CO_2 observed in this study suggest that the majority of CO_2 is transported into these caves as a gas and not dissolved in water. If carbon isotope equilibrium is maintained between CO_2 and DIC during degassing from the water, the $\delta^{13}C$ value of the first CO_2 emitted into the cave atmosphere would equal $\delta^{13}C_s$ not the $\delta^{13}C$ value of CO_2 respired in the soil ($\delta^{13}C_{r\text{-soil}}$; because the water equilibrated in the epikarst with pore space CO_2, not respired CO_2). The $\delta^{13}C$ value of degassed CO_2 would increase with the fraction of total carbon degassed because $\alpha_{CO_2\text{–}HCO_3^-} < 1$; 100% degassing would result in cave-air CO_2 $\delta^{13}C_r$ values equal to the $\delta^{13}C$ value of DIC in equilibrium with soil CO_2. The occurrence of kinetic isotope effects during degassing would result in $\delta^{13}C_r$ values of cave-air CO_2 that are lower than $\delta^{13}C_r$ values of soil CO_2, as observed in IS during the winter. Therefore, the observed similarity between tree-dominated soil and cave $\delta^{13}C_r$ values requires either (1) equilibrium degassing of a small fraction of cave water DIC and advective mixing of cave-air to prevent carbon isotope fractionation by diffusion of CO_2 or (2) transport of CO_2 into caves as a gas. Under conditions required for (1), all speleothem calcite might precipitate in isotope equilibrium with soil CO_2 and vadose water, which would be ideal for paleoclimate reconstruction. We, however, think (2) is more likely, given evidence presented here and previously for kinetic isotope fraction during degassing of CO_2 from cave drip waters (e.g. Spötl et al., 2005) Precise measurement of oxygen concentrations in cave-air would help distinguish between CO_2 transport into caves in water or as a gas (Halbert, 1982). Depletions of O_2 in cave-air

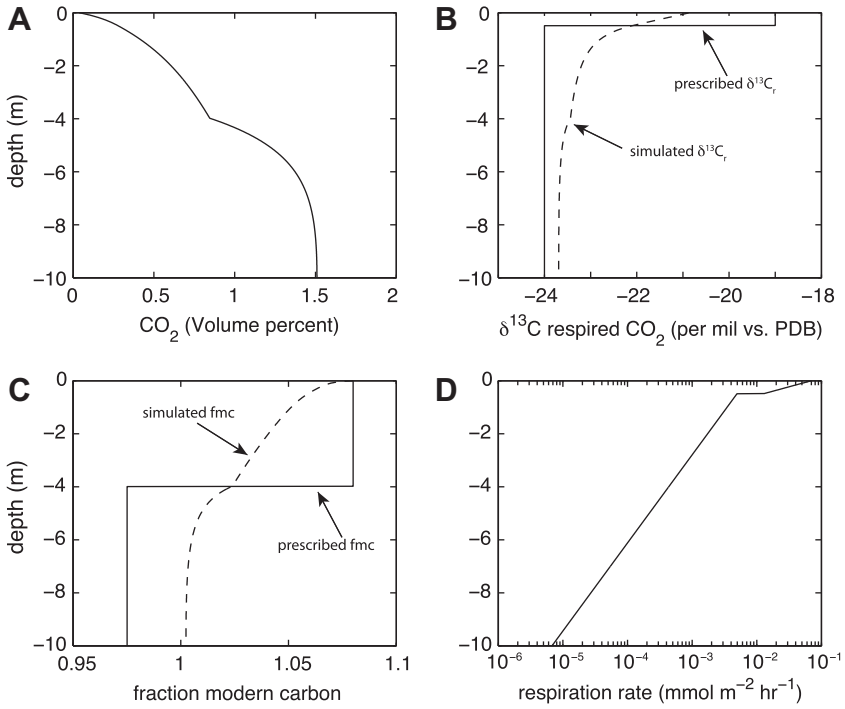

Fig. 5. Simulations of pore space CO_2 in a 10 m column of soil and epikarst. A numerical production-diffusion model was used to simulate steady-state profiles of CO_2. (A) CO_2 concentrations, (B) $\delta^{13}C$ values of respired CO_2. The solid line shows values prescribed as model input; the dashed line shows simulated $\delta^{13}C_r$ values calculated from model output using equation 1 from the text. The simulated $\delta^{13}C_r$ values can be compared with $\delta^{13}C_r$ values calculated from measured concentrations and $\delta^{13}C$ values of soil and cave-air CO_2. (C) The fraction modern carbon (fmc) in pore space CO_2. The solid line shows values prescribed as model input; the dashed line shows values calculated from model output. (D) Respiration rates used as model input. Free air porosity was prescribed as follows: 0–0.5 m, porosity = 0.5; 0.5–2 m, porosity = 0.3; 2–10 m, porosity = 0.1. The tortuosity factor and temperature were held constant at 0.6 and 15 °C, respectively. CO_2 respired below 4 m was assigned a fmc of 0.87, equivalent to the fmc in 2009 of organic carbon removed from the atmosphere in 1000 A.D.

below tropospheric O_2 concentrations that balance the enrichment of cave-air CO_2 above tropospheric CO_2 concentrations would indicate gas phase transport between soil and cave whereas elevated cave-air CO_2 concentrations without compensatory O_2 consumption would indicate that CO_2 enters caves by degassing from water.

6.4. Seasonal variation of cave-air CO_2

The concentration of CO_2 in the cave atmosphere at a given point in time is the result of a balance between CO_2 fluxes into the cave from external sources and CO_2 fluxes out by removal mechanisms. Seasonal variations in cave-air CO_2 are the result of fluctuations in the magnitude of these fluxes. However, it is difficult to conclusively determine the dominant cause of cave-air CO_2 change because the source and sink strengths both change seasonally. $\delta^{13}C$ values alone are insufficient to distinguish between a reduced soil respiration flux or increased ventilation because both processes would result in an increased tropospheric CO_2 to soil-respired CO_2 ratio and therefore higher cave-air CO_2 $\delta^{13}C$ values.

Wong and Banner (2010) investigated the effects of vegetation removal over cave NBS. Their work provides an indirect means of resolving whether changes in soil respiration rate or changes in ventilation strength have a larger effect on cave-air CO_2. Cave-air CO_2 was measured over a period of 5 years: 2 years with natural surface vegetation followed by 3 years over which a large portion of vegetation cover, primarily Juniper trees, above a section of the cave was removed (Wong and Banner, 2010). Within NBS, they found immediate and significant decreases in cave-air CO_2 concentrations and dampened summer CO_2 concentrations in the years following vegetation removal. The large effects of vegetation removal on cave-air CO_2 suggest that root respiration, specifically juniper root systems, are a significant source of CO_2 to the cave (Wong and Banner, 2010). This is consistent with our interpretations based on carbon isotope ratios of cave and soil CO_2. The lack of any observable response of cave-air CO_2 to brush removal during the winter months suggests that winter CO_2 deceases are primarily controlled by CO_2 removal through ventilation rather than decreases in soil respiration rate. It follows that soil/epikarst respiration controls how high CO_2 gets during the summer months and that density-driven ventilation controls how low CO_2 gets during the winter months. Lower summer cave-air CO_2 concentrations in IS than in the other caves may be the result of the shallow depths of respiration in the grassland-dominated soils above the cave or to the occasional use of ventilation shafts.

If all other factors are held equal, then shallower depths of respiration results in lower pore space CO_2

concentrations. Therefore, when compared with other caves we studied, shallow depths of respiration in the contiguous grasslands above IS may explain the lower summer maximum CO_2 concentrations in this cave. Furthermore, the presence of contiguous grassland and the associated shallow respiration might limit speleothem growth rates because epikarst CO_2 concentrations control the maximum Ca^{2+} concentrations of water entering caves. Likewise, temporal variation in the rooting depth of vegetation might influence the growth rate of speleothems through time.

6.5. Diurnal cave-air CO_2 cycle

Lateral transects into IS suggest that distinct air masses identifiable using measured $\delta^{13}C$ values and CO_2 concentrations exist within the cave (Fig. 4). The air mass furthest from the entrance of the cave, and closest to the woodland vegetation above the cave, has a $\delta^{13}C_r$ value of approximately $-23‰$ whereas an air mass in the vicinity of ISST has a $\delta^{13}C_r$ value about 1‰ higher (Fig. 4). The air mass closest to the entrance has an intermediate $\delta^{13}C_r$ value. The transitions between these air masses are relatively abrupt (~75 m) and their positions within the cave oscillate with a period of approximately 24 h; the transitions were furthest from the entrance at 7:00 and closest to the entrance at 13:00 (CST) during our 24 h monitoring study. Movement of the transitions between the air masses across sites ISPT and ISHW results in diurnal variation in $\delta^{13}C_r$ values at individual locations, which are especially pronounced at ISPT (Fig. 4). This diurnal movement of the air in and out of the cave is likely controlled by atmospheric tides (Volland, 1997) as concluded by Cowan (2010) for central Texas caves, whereby decreases in atmospheric pressure pull air from deeper in a cave toward its entrance and vice versa. The differences in $\delta^{13}C_r$ values among the air masses in IS likely result from differences in vegetation above the cave. The vegetation at the entrance to the cave is dominated by forbs and oak trees (Table 3 and Fig. 1) and a patch of woodland occurs above site ISLM, whereas mid-cave-air mass with relatively high $\delta^{13}C_r$ values is under grassland and Interstate Highway 35.

7. CONCLUSIONS

(1) CO_2 is transported as a gas into the caves studied, except in Inner Space Cavern during the winter when a significant amount of CO_2 degasses from cave water. Calculating $\delta^{13}C$ values of respired CO_2 is therefore useful for investigating the sources of CO_2 in cave-air.
(2) Deeply rooted vegetation, if present, supplies the majority of the CO_2 to caves even if the rates of deep respiration are low and the fraction of surface cover by deeply rooted plants is small, especially if the epikarst has a low porosity.
(3) The distribution of vegetation is more important than the fraction of coverage in determining the relative contribution of CO_2 from different types of plants to cave-air. Large contiguous areas of shallowly rooted vegetation can overcome the bias against shallow respiration in the $\delta^{13}C$ value of deep pore space CO_2.
(4) Oxidation of old organic matter in the epikarst or equilibration of cave-air with large volumes of old groundwater may result in radiocarbon activities of cave-air CO_2 that are lower than the activities in soil CO_2.
(5) Variations in the $\delta^{13}C$ value of CO_2 in cave-air support the ideas that density-driven ventilation is a sink for cave-air CO_2 during the winter and that diurnal barometric pumping during the summer shifts air mass inside caves.

These considerations lay the groundwork for more accurate interpretations of speleothem-based paleoclimate proxies, particularly the carbon isotope composition of speleothem calcite.

ACKNOWLEDGMENTS

We thank the owners and staff at Inner Space Cavern and Natural Bridge Caverns for access, and the Texas Cave Management Association for access to Whirlpool Cave. We also thank T. Quinn for instrument time, N. Fowler for assistance with plant identification at IS and NB and J. Bowers and T. Fisher for assistance with plant identifications at Cave of the Bells. This research was supported by NSF REU Grant EAR-0852029, NSF P2C2 Grant ATM-0823665 and the Geology Foundation and the Environmental Science Institute of the University of Texas at Austin.

REFERENCES

Baker A. and Genty D. (1998) Environmental pressures on conserving cave speleothems: Effects of changing surface land use and increased cave tourism. *J. Environ. Manage.* **53**, 165–175.

Baker A., Ito E., Smart P. L. and McEwan R. F. (1997) Elevated and variable values of ^{13}C in speleothems in a British cave system. *Chem. Geol.* **136**, 263–270.

Baldini J. U. L., Baldini L. M., McDermott F. and Clipson N. (2006) Carbon dioxide sources, sinks, and spatial variability in shallow temperature zone caves: Evidence from Ballynamintra Cave, Ireland. *J. Cave Karst Stud.* **68**, 4–11.

Baldini J. U. L., McDermott F., Hoffmann D. L., Richards D. A. and Clipson N. (2008) Very high-frequency and seasonal cave atmosphere pCO_2 variability: Implications for stalagmite growth and oxygen isotope-based paleoclimate records. *Earth Planet. Sci. Lett.* **272**, 118–129.

Banner J. L., Guilfoyle A., James E. W., Stern L. A. and Musgrove M. (2007) Seasonal variations in modern speleothem calcite growth in central Texas, U.S.A. *J. Sediment. Res.* **77**, 615–622.

Bar-Matthews M., Ayalon A., Kaufman A. and Wasserberg G. J. (1999) *The Eastern Mediterranean Plaeoclimate as a Reflection of Regional Events*. Soreq Cave, Israel.

Batiot-Guilhe C., Seidel J.-L., Jourde H., Hébrard O. and Bailly-Comte V. (2007) Seasonal variations in CO_2 and ^{222}Rn in a Mediterranean sinkhole – Spring (Causse d'Aumelas, SE France). *Int. J. Speleol.* **36**, 51–56.

Bird R. B., Stewart W. E. and Lightfoot E. N. (1960) *Transport Phenomena*. John Wiley, New York, p. 780.

Breecker D. and Sharp Z. D. (2008) A field and laboratory method for monitoring the concentration and stable isotope composition of soil CO_2. *Rapid Commun. Mass Spectrom.* **22**, 449–454.

Brown J. R. and Archer S. R. (1990) Water relations of a perennial grass seedling vs adult woody plants in a subtropical savanna, Texas. *Oikos* **57**, 366–374.

Buecher R. H. (1999) Microclimate study of Kartchner Caverns, Arizona. *J. Cave Karst Stud.* **61**, 108–120.

Cerling T. E. (1984) The stable isotopic composition of modern soil carbonate and its relationship to climate. *Earth Planet. Sci. Lett.* **71**, 229–240.

Cerling T. E., Solomon D. K., Quade J. and Bowman J. R. (1991) On the isotopic composition of carbon in soil carbon dioxide. *Geochim. Cosmochim. Acta* **55**, 3403–3405.

Cooke M. J., Stern L. A., Banner J. L. and Mack L. E. (2007) Evidence for the silicate source of relict soils on the Edwards Plateau, central Texas. *Quatern. Res.* **67**, 275–285.

Cowan B. D. (2010) Temporal and spatial variability of cave-air CO_2 in central Texas. MS thesis, Univ. of Texas, Austin.

Cowan B. D., Osborne M. C. and Banner J. L. (in press) Temporal variability of cave-air CO_2 in central Texas. *J. Cave Karst Stud.*

Craig H. (1954) The geochemistry of the stable carbon isotopes. *Geochim. Cosmochim. Acta* **3**, 53–92.

Davidson G. R. (1995) The stable isotope composition and measurement of carbon in soil CO_2. *Geochim. Cosmochim. Acta* **59**, 2485–2489.

Davis O. K. (1994) The Correlation of summer precipitation in the southwestern U.S.A. with isotopic records of solar activity during the medieval warm period. *Clim. Change* **26**, 271–287.

de Freitas C. R., Littlejohn R. N., Clarkson T. S. and Kristament I. S. (1982) Cave climate: Assessment of airflow and ventilation. *J. Climatol.* **2**, 383–397.

Denniston R. F., DuPree M., Dorale J. A., Asmerom Y., polyak V. J. and Carpenter S. J. (2007) Episodes of late Holocen aridity recorded by stalagmites from Devil's Icebix Cave, central Missouri, USA. *Quatern. Res.* **68**, 45–52.

Dorale J. A., Gonzalez L. A., Reagan M. K., Pickett D. A., Murrell M. T. and Baker R. G. (1992) A high-resolution record of Holocene climate change in speleothem calcite from Cold Water Cave, northeast Iowa. *Science* **258**, 1626–1630.

Dorale J. A., Edwards R. L., Ito E. and González L. A. (1998) Climate and vegetation history of the midcontient from 75 to 25 ka: A speleothem record from Crevice Cave, Missouri, USA. *Science* **282**, 1871–1874.

Dulinski M. and Rozanski K. (1990) Formation of $^{13}C/^{12}C$ isotope ratios in speleothems; a semi-dynamic model. *Radiocarbon* **32**, 7–16.

Dykoski C. A., Edwards R. L., Cheng H., Daoxian Y., Cai Y., Meilian Z., Lin Y., Qing J., An Z. and Revenaugh J. (2005) A high-resolution absolute-dated Holocene and deglacial Asian monsoon record from Dongge Cave, China. *Earth Planet. Sci. Lett.* **233**, 71–86.

Ek C. and Gewalt M. (1985) Carbon dioxide in cave atmospheres: New results in Belgium and comparison with some other countries. *Earth Surf. Proc. Land.* **10**, 173–187.

Elliot W. R., Veni G. (1994) The Caves and Karst of Texas – 1994 NSS Convention Guidebook.

Fairchild I., Smith C. L., Baker A., Fuller L., Spötl C., Mattey D., McDermott F. and E.I.M.F. (2006) Modification and preservation of environmental signals in speleothems. *Earth Sci. Rev.* **75**, 105–153.

Frisia S., Fairchild I. J., Fohlmeister J., Miorandi R., Spötl C. and Borsato A. (2011) Carbon mass-balance modelling and carbon isotope exchange processes in dynamic caves. *Geochim. Cosmochim. Acta* **75**, 380–400.

Gascoyne M. (1992) Paleoclimate determination from cave calcite deposits. *Quatern. Sci. Rev.* **11**, 609–632.

Genty D., Blamart D., Ouahdi R., Gilmour M., Baker A. and Jouzel van Exter S. (2003) Precise dating of Dansgaard-Oeschger climate oscillations in western Europe from stalagmite data. *Nature* **421**, 833–837.

Godfrey C. L., Kckee G. S. and Oakes H. (1973) General Soil Map of Texas: Texas Agricultural Experimental Station. Texas A&M University, in cooperation with the Soil Conservation Service, US Department of Agriculture.

Halbert E. J. M. (1982) Evaluation of carbon dioxide and oxygen data in cave atmospheres using the Gibbs triangle and the cave-air index. *Helictite* **20**, 60–68.

Hellstrom J., McCulloch M. and Stone J. (1998) A detailed 31,000-year record of climate and vegetation change, from the isotope geochemistry of two New Zealand speleothems. *Quatern. Res.* **50**, 167–178.

Hoffman D. L., Beck J. W., Richards D. A., Smart P. L., Singarayer J. S., Ketchmark T. and Hawkesworth C. J. (2010) Towards radiocarbon calibration beyond 28 ka using speleothems from the Bahamas. *Earth Planet. Sci. Lett.* **289**, 1–10.

Jackson R. B., Moore L. A., Hoffman W. A., Pockman W. T. and Linder C. R. (1999) Ecosystem rooting depth determined with caves and DNA. *Proc. Natl. Acad. Sci. USA* **96**, 11387–11392.

James J. M. (1977) Carbon dioxide in the cave atmosphere. *Trans. Br. Cave Res. Assoc.* **4**, 417–429.

Jost W. (1960) *Diffusion in Solids, Liquids, Gases*. Academic Press, New York, NY.

Kowalczk A. J. and Froelich P. N. (2010) Cave-air ventilation and CO_2 outgassing by radon-222 modeling: How fast do caves breathe? *Earth Planet. Sci. Lett.* **289**, 209–219.

Leavitt S. W. (1994) Major wet interval in the White Mountains medieval warm period evidenced in $\delta^{13}C$ of bristlecone pine tree rings. *Clim. Change* **26**, 299–307.

Meyer K. (2011) Southwest U.S. paleoclimate over the past 30 ky: Insights from speleothem $\delta^{18}O$ and growth rate time series. MS thesis, Univ. of Texas.

Mickler P. J., Stern L. A. and Banner J. L. (2006) Large kinetic isotope effects in modern speleothems. *Geol. Soc. Am. Bull.* **118**, 65–81.

Musgrove M., Banner J. L., Mack L. E., Combs D. M., James E. W., Cheng H. and Edwards R. L. (2001) Geochronology of late Pleistocene to Holocene speleothems from central Texas: Implications for regional paleoclimate. *Geol. Soc. Am. Bull.* **113**, 1532–1543.

Nobel P. S. (1988) *Environmental Biology of Agaves and Cacti*. Cambridge University Press, Cambridge.

O'Brien B. J. and Stout J. D. (1978) Movement and turnover of soil organic matter as indicated by carbon isotope measurements. *Soil Biol. Biochem.* **10**, 309–317.

Oster J. L., Montañez I. P., Sharp W. D. and Cooper K. M. (2009) Late Pleistocene California droughts during deglaciation and Artic warming. *Earth Planet. Sci. Lett.* **288**, 434–443.

Oster J. L., Montañez I. P., Guilderson T. P., Sharp W. D. and Banner J. L. (2010) Modeling speleothem $\delta^{13}C$ variability in a central Sierra Nevada Cave using ^{14}C and $^{87}Sr/^{86}Sr$. *Geochim. Cosmochim. Acta* **74**, 5228–5242.

Oster J. L., Montañez I. P. and Kelley N. P. (2012) Response of a modern cave system to large seasonal precipitation variability. *Geochim. Cosmochim. Acta* **91**, 92–108.

Quade J., Cerling T. E. and Bowman J. R. (1989) Systematic variations in the carbon and oxygen isotopic composition of pedogenic carbonate along elevation transects in the

southern Great Basin, United States. *Geol. Soc. Am. Bull.* **101**, 464–475.

Richards D. A. and Dorale J. A. (2003) Uranium series chronology and environmental application of speleothems, in Uranium Series Geochemistry. *Rev. Mineral. Geochem.* **52**, 407–460.

Rudzka D., McDermott F., Baldini L. M., Fleitmann D., Moreno A. and Stoll H. (2011) The coupled δ^{13}C-radiocarbon systematics of three Late Glacial/early Holocene speleothems; insights into soil and cave processes at climatic transitions. *Geochim. Cosmochim. Acta* **75**, 4321–4339.

Schoeller D. A., Klein P. D., Watkins J. B., Heim T. and MacLean, Jr., W. C. (1980) ^{13}C abundances of nutrients and the effect of variations in ^{13}C isotopic abundances of test meals formulated for $^{13}CO_2$ breath tests. *Am. J. Clin. Nutr.* **33**, 2375–2385.

Southon J., Noronha A. L., Cheng H., Edwards R. L. and Wang Y. (2012) A high-resolution record of atmospheric ^{14}C based on Hulu Cave speleothems. *Quatern. Sci. Rev.* **33**, 32–41.

Spötl C., Fairchild I. J. and Tooth A. F. (2005) Cave-air control on dripwater geochemistry, Obir Caves (Austria): Implications for speleothem deposition in dynamically ventilated caves. *Geochim. Cosmochim. Acta* **69**, 2451–2468.

Stuiver M. and Polach H. A. (1977) Reporting of ^{14}C data. *Radiocarbon* **3**, 355–363.

Troester J. W. and White W. B. (1984) Seasonal fluctuations in the carbon dioxide partial pressure in a cave atmosphere. *Water Resour. Res.* **20**, 153–156.

Trolier M., White J. W. C., Tans P., Masarie K. A. and Gemery P. A. (1996) Monitoring the isotopic composition of atmospheric CO_2: Measurements from the NOAA Global Air Sampling Network. *J. Geophys. Res.* **101**, 25,897–25,916.

Volland H. (1997) Atmopsheric tides. In Tidal Phenomena, Lecture Notes in Earth Sciences 66, (eds. H. Wilhelm W. Zürn, and H.-G. Wenzel). Springer-Verlag, Berlin-Heidelberg, 221–246.

Wagner J. D. M., Cole J. E., Beck J. W., Patchett P. J., Henderson G. M. and Barnett H. R. (2010) Moisture variability in the southwestern United States linked to abrupt glacial climate change. *Nat. Geosci.* **3**, 110–113.

Wang Y. G., Cheng H., Edwards R. L., An Z. S., Wu J. Y., Shen C.-C. and Dorale J. A. (2001) A high-resolution absolute-dated late Pleistocene monsoon record from Hulu Cave, China. *Science* **294**, 2345–2348.

White W. B. (1988) *Geomorphology and Hydrology of Karst Terrains*. Oxford University Press, New York.

Wigley T. M. L. and Brown M. C. (1976) The physics of caves. In *The Science of Speleology* (eds. T. D. Ford and C. H. D. Cullingford). Academic Press, London, pp. 329–345.

Wood W. W. (1985) Origin of caves and other solution openings in the unsaturated (vadose) zone of carbonate rocks: A model for CO_2 generation. *Geology* **13**, 822–824.

Wong C. and Banner J. L. (2010) Response of cave-air CO_2 and drip water to brush clearing in central Texas: Implications for recharge and soil CO_2 dynamics. *J. Geophys. Res.* **115**, G04018.

Associate editor: Jerome Gaillardet